The unknotted strands of life: knots are very rare in RNA structures

C. Micheletti[1], M. Di Stefano[1] and H. Orland[2]
[1] *SISSA - Scuola Internazionale Superiore di Studi Avanzati, Via Bonomea 265, 34136 Trieste (Italy)*
[2] *Institut de Physique Théorique, CEA-Saclay, CEA 91191 Gif-sur-Yvette, France*
(Dated: October 4, 2014)

The ongoing effort to detect and characterize physical entanglement in biopolymers has so far established that knots are present in many globular proteins and also abound in viral DNA packaged inside bacteriophages. RNA molecules, on the other hand, have not yet been systematically screened for the occurrence of physical knots. We have accordingly undertaken the systematic profiling of the ∼6,000 RNA structures present in the protein data bank. The search identified no more than three deeply-knotted RNA molecules. These are ribosomal RNAs solved by cryo-em and consist of about 3,000 nucleotides. Compared to the case of proteins and viral DNA, the observed incidence of RNA knots is therefore practically negligible. This suggests that either evolutionary selection, or thermodynamic and kinetic folding mechanisms act towards minimizing the entanglement of RNA to an extent that is unparalleled by other types of biomolecules. The properties of the three observed RNA knotting patterns provide valuable clues for designing RNA sequences capable of self-tying in a twist-knot fold.

PACS numbers:

arXiv:1410.1549v1 [q-bio.BM] 6 Oct 2014

I. INTRODUCTION

The notion that biomolecules should be minimally entangled, so as to fold efficiently and reproducibly and sustain functionally-oriented structural arrangements, appears so intuitive that viable biological molecules have long been thought to be free of physical knots[1].

Indeed, only several years after the publication of the human carbonic anhydrase II structure [2] was it realized that the enzyme backbone was tied in a trefoil knot [3]. More and more instances of knotted and slipknotted proteins have since been discovered[4, 5], and it is now established that about 2% of the protein chains deposited in the PDB host physical knots [1, 6]. The latter range in complexity from the simplest trefoil knot to the six crossing Stevedore's knot [7].

The functional implications of these knots are still unclear. Nevertheless, several hypotheses have been formulated to rationalize the functional advantage that arguably leads specific knotted proteins to evolve from unknotted ones [6, 8]. For instance, knots have been argued to enhance the mechanical stability of active sites and preventing proteolytic degradation [8, 9].

While empirical evidence demonstrates *de facto* that knotted proteins do exist it also confirms the expectations that physical knots can significantly hinder and slow down the spontaneous folding process[10]. This is because the various folding steps need to be well coordinated to ensure the formation of the correct knot type in the correct protein location[11–13]. This limited kinetic accessibility is likely responsible for the much lower incidence of knots in proteins compared to generic equilibrated polymers [14], where entanglement inevitably arises with increasing chain length and compactness [15–18].

Physical knots have also been shown to occur abundantly in the double-stranded DNA (dsDNA) of a number of viruses [19–21]. For instance, a series of remarkable experiments carried out on the bacteriophage P4 [21–23] have shown that its 10kbp-long dsDNA contains many more physical knots when packaged inside the phage capsid than when free in solution [24]. In fact, the P4 genome has a 95% probability of accommodating complex physical knots [21–23, 25] when it is packaged inside a viral particle where it cannot be simplified by topoisomerases[26, 27].

As for the case of proteins, the discovery of knots in packaged viral DNA raised several questions about their functional implications, particularly for the expected difficulty of ejecting the knotted genome from the narrow capsid exit pore. More recent studies have shown that this conundrum can be solved by considering the working of topological friction at the molecular scale [28] and especially the ordering effect of DNA self-interactions [25] which favours the untying of DNA knots inside the capsid during ejection [29].

Nowadays, the occurrence of physical entanglement in proteins and DNA, is not only well-documented but is characterized well enough that novel knotted proteins and short DNA molecules have been successfully designed and the average entanglement of DNA filaments can be created or relaxed in a controlled manner[30–32].

These topological profiling efforts, however, have not been paralleled for the third and last kind of strand of life[33], namely RNA. To the best of our knowledge no systematic survey of physical knots in RNAs has been carried out so far and no physical knots have been reported in naturally-occurring RNA structures.

The interest in characterizing and detecting other forms of RNA entanglement has nevertheless been significant in past years, particularly regarding pseudo-knots. These are secondary structure elements with a non-trivial geometry which abound in RNA molecules and which can have important functional implications [34–37]. In particular, several efforts are being spent to clarify how ex-

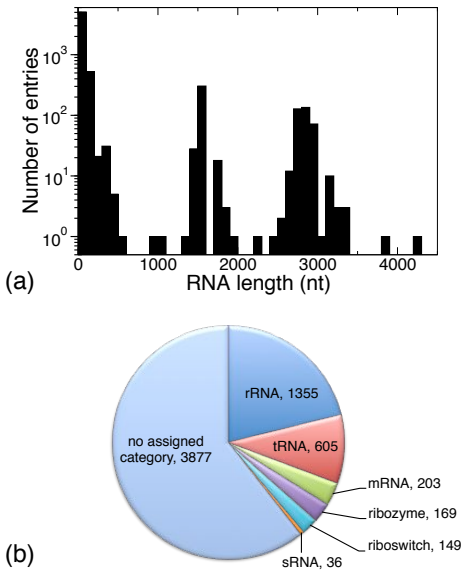

FIG. 1: RNA dataset properties. The length distribution and categorized subdivision of the considered RNA chains are given in panels (a) and (b), respectively. The category assignment is based on the COMPND field of the the PDB structure files.

actly pseudoknots can hinder RNA translocation through the ribosomal pore and cause a shift in the codon reading frame [36, 38–40].

Qualitatively however, pseudoknots are very different from physical knots. In fact, as their name suggest, they are not real knots: by pulling on the ends of a chain, any pseudoknot will progressively yield until the chain is fully stretched, while physical knots will never disappear but rather tighten up.

Clearly, the impact of knots on RNA mechanical resistance, and hindrance to translocation can be much more dramatic than that of pseudoknots, and hence establishing their degree of occurrence can shed light on their biological relevance and implications.

In this respect it is important to recall the seminal study of Wang *et al.* [41], who succeeded in designing an RNA sequence of 104 nucleotides capable of folding into a knotted structure. The study not only gave a proof of concept that RNA can be knotted, but also established that the *Escherichia coli* DNA topoisomerase III could catalyze the interconversion of knotted and unknotted forms of the synthetic RNA. Clearly, the very existence of enzymes acting as RNA topoisomerases points to their putative role in simplifying RNA entanglement, including knots, *in vivo*. As a matter of fact, the recently discovered eukaryotic circular RNAs (circRNAs) [42–45] have been argued to be good candidates for hosting knots which could be permanently trapped by their circular structure [46].

II. RESULTS AND DISCUSSION

These considerations motivated us to carry out a systematic search for the occurrence of physical knots on all the RNA structures that are presently available in the protein data bank (PDB)[47].

To this purpose we considered all currently available PDB entries and isolated 2,863 of them which involve RNA either alone or in association with proteins and DNA or hybridized with DNA. The total number of distinct RNA chains extracted from these entries was equal to 6,394. The length distribution of the considered RNA chains and their categorized subdivision is given in Fig. 1.

The backbone (P-atoms trace) of each RNA chain was circularized "in silico" using the so-called minimally-interfering closure scheme[48]. This algorithm turns the linear, open, backbone of the molecule into a closed structure which hence has a mathematically well-defined topological state. The knotted state of the closed backbone was finally established by computing its Dowker code which is a non-ambiguous topological indicator that can be used to identify prime knots of up to 16 crossings by comparison against available look-up tables, see Methods.

In our systematic survey we found only three instances of RNA molecules that accommodate physical knots in their structurally-intact (no breaks) backbone. The properties of these knotted structures are given in Table 1, where they are listed in order of increasing topological complexity and chain length.

The first instance corresponds to the figure-of-eight or Flemish knot, 4_1, and is found in the *Escherichia coli* 23S ribosomal RNA. The second instance is a much more complex 16-crossings prime knot which is present in the *Thermomyces lanuginosus* 26S ribosomal unit. The two molecules consist of about $2,800$ and $3,200$ nucleotides, respectively. Finally, the third knotted structure is, again, an *Escherichia coli* 23S ribosomal RNA. Unlike the first instance, however, it features a composite knot formed by the succession of four separate prime knotted components: three trefoil knots plus a figure-of-eight knot.

We start by discussing the complex knot found for the 26S ribosomal unit, which is shown in Fig. 2. In this figure, panel (a) represents the whole molecule, while the "essential" knotted region is shown in panels (b) and (c). This essential region was obtained by shortcutting helices that do not contribute to the topological entanglement of the molecule, so as to make its knotted state readily perceivable by visual inspection. Panel (d), instead, is a minimal diagrammatic representation of the closed physical knot. As it is apparent from panels (c) and (d), the high nominal complexity of this entanglement, which is measured through the number of crossings in the simplest diagrammatic projection, mostly arises because of the clasp formed by two helices located at the top of panel (c). The nucleotides at the clasp have a large sequence separation, about 2,000 nucleotides, which underscores

Knot	Molecule	Organism	# nucleotides	PDB ID	Essential knotted region	Essential crossings
4_1	23S rRNA	*Escherichia coli*	2,740	2GYA:0	A1434–U1563	G1478–C1480 and C1558–C1561
16_{124834}	26S rRNA	*Thermomyces lanuginosus*	3,170	3JYX:5	A416–A428, G616–C636, A647–A677, C700–G716, G787–A791, A1373–A1433, U1439–U1448, C2389–C2405, G2619–C2625, C2760–U2822, U2978–U2999	C618–A622 and A1401–U1405 A710–G714 and U2775–A2780
$3_1\#3_1\#4_1\#3_1$	23S rRNA	*Escherichia coli*	2,904	1C2W:B	G254-C366 (3_1) G520-A825 (3_1) U1440-A1535 (4_1) U1851-C1892 (3_1)	G263–C264 and G363–C364 C581–G583 and C814–C816 C1454–G1455 and C1526–G1527 U1476–A1477 and G1514–A1515 U1856–G1857 and C1887–G1888

TABLE I: **Knotted RNA structures** For the 23S knotted units the knotted regions correspond to relatively short, uninterrupted stretches of the backbone which accommodate the whole knot (for 2GYA:0) or its separable prime components (for 1C2W:B), see Figs. 3 and 4. To expose with maximum clarity the more delocalised knot of the 26S unit 3JYX:5, we list the sequence of backbone segments that, once joined, embody the fundamentally-entangled portion of this molecule, see Fig. 2. Such essential knotted region was obtained by "shortcutting" nugatory helices and loops that do not contribute to the chain entanglement. The essential crossings consist of pairs of facing RNA strands which can untie or simplify the knot when passed through each other. The nucleotide numbering follows the indexing of the associated PDB file.

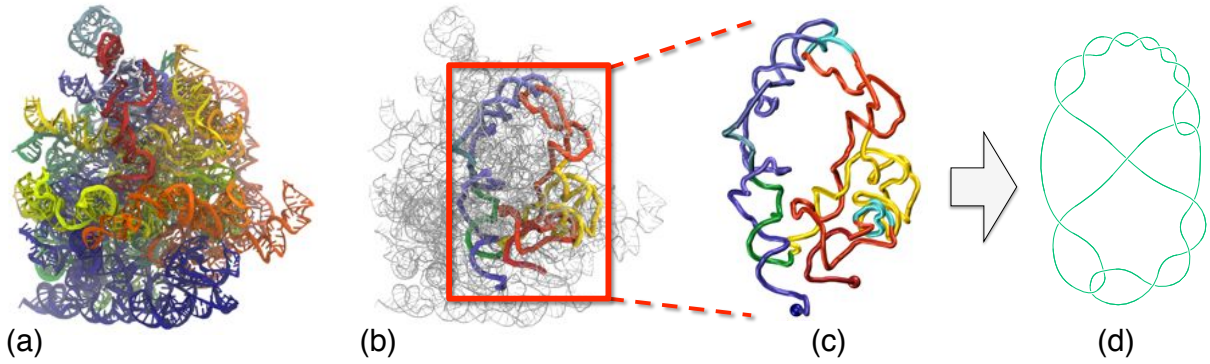

FIG. 2: Knotted 26S ribosomal RNA structure from PDB entry 3JYX:5. The complete structural representation of the RNA chain is given in panel (a) and is colored according to a rainbow scheme, red → yellow → green → blue, across the two termini. The essential knotted region, tied in a 16-crossings knot, is highlighted in panel (b) and is presented in excerpted form in panel (c). The short cyan regions in panel (c) highlight the essential crossings of the knot, see Table 1. The minimal ring diagram of the corresponding 16-crossings knot is shown in panel (d).

the significant non-locality of the knot. It is important to notice that the knot would persist even if this clasp was removed by a suitable strand passage. In fact, in this case, the original sixteen-crossings knot would simplify to a seven-crossing one (7_2) which can finally be untied by a further virtual strand passage. The two regions which are arguably naturally primed for such simplifying strand-passages are listed in Table 1 and highlighted in cyan in panel (c).

We now turn to the two knotted 23S units from *Escherichia coli*, starting from chain 2GYA:0 which is shown in Fig. 3a. The entangled region of this molecule spans as few as 150 nucleotides and its knotted state, corresponding to a simple figure-of-eight (4_1) knot, is clearly seen in the excerpted knotted region of Fig. 3c. The featured figure-of-eight knot is an achiral twist knot. These kind of knots are easily produced by a single strand passage in rings that are repeatedly twisted. It is intriguing to notice: (i) the analogy of this mechanism with the strand passages occurring in RNA helices as in the previous case and (ii) this mechanism is utterly different from the one emerging in densely packed double-stranded DNA, where torus knots are abundant and twist knots rare[22, 23]. Unlike the discussed 26S case, a single strand passage suffices to untie the observed 4_1 knot. A possible essential crossing, where the untying strand passage could be performed, is listed in Table 1 and highlighted in red in Fig. 3c.

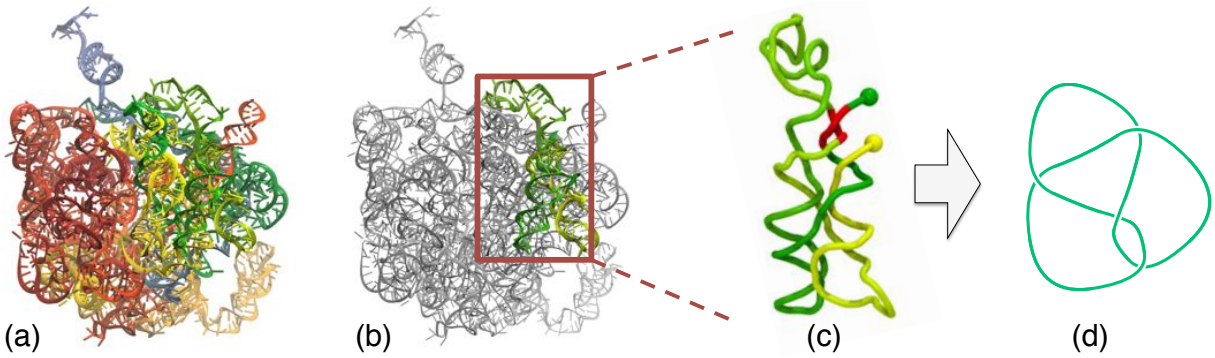

FIG. 3: Knotted 23S ribosomal RNA structure from PDB entry 2GYA:0. The complete structural representation of the ribosomal structure is given in panel (a) and is colored according to a rainbow scheme across the two termini. The knotted region, tied in a figure-of-eight or 4_1 knot, is highlighted in panel (b) and is presented in excerpted form in panel (c). The red regions in panel (c) highlight the essential crossing of the knot, see Table 1. The minimal ring diagram of the figure-of-eight knot is shown in panel (d).

The other knotted instance of the 23S unit, corresponding to the 1C2W:B chain, is finally shown in Fig. 4. It features a composite knot resulting from the concatenation of four separate prime components: a figure-of-eight knot and three trefoil ones, see Fig. 4b. The entanglement of the shortest component, which consists of only ~ 40 nucleotides is clearly visible in the backbone trace of Fig. 4c.

In connection with RNA self-entanglement, it is worth recalling that it has been proposed to classify RNA structures by their topological genus [49, 50]. The genus provides a useful characterization of the complexity of pseudoknots and can be used for secondary structure prediction [51, 52]. It is thus interesting to ascertain if it correlates with the nominal complexity of the knots found in the RNA. Accordingly, we used the RNApdbee web server [53], to extract the secondary structures of the RNA from their PDB files and then computed the corresponding genii using the computational engine of the McGenus web server [52]. We found that the two 23S ribosomal units, 2GYA:0 and 1C2W:B, have genus respectively equal to $g = 6$ and $g = 7$, while the knotted 26S ribosomal unit has genus equal to $g = 5$. As was shown in [50], these genii are fairly small, but still compatible with the typical size of $3,000$ nucleotides of these RNAs.

The fact that only three RNA molecules are knotted over a set of about $6,000$ entries indicates the extreme paucity of non-trivial entanglement in naturally-occurring RNAs. As a matter of fact, the knots incidence is so low that one may doubt whether the three exceptional structures are genuinely knotted.

This point is particularly pertinent because both the 23S and 26S ribosomal RNAs were solved by cryo-electron microscopy (cryo-em). This technique has proved invaluable for gaining quantitative insight into the structural organization of large and complex biomolecular structures, including the three knotted instances discussed here. At the same time, its scope can be limited in practice by two main factors. First, the electronic flux impacting the molecules may be high enough to alter their structures. Secondly, the resolution of cryo-em maps is appreciably lower than in conventional crystallography and hence is prone to ambiguous model reconstruction without suitable knowledge-based constraints. For a better control of the latter ambiguities, several order parameters are usually monitored to establish the local quality of the model fit of the electron density map.

Such quality parameters are available for PDB entries 2GYA:0 and 3JYX:5. In both cases, it is found that the regions corresponding to the knots' "essential crossings"

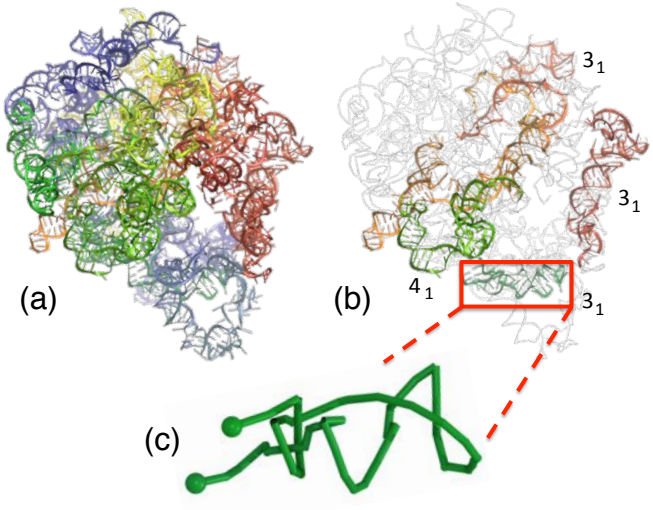

FIG. 4: Knotted 23S ribosomal RNA structure from PDB entry 1C2W:B. The complete structural representation of the RNA chain is given in panel (a) and is colored according to a rainbow scheme across the two termini. The four prime components of the knotted region are highlighted in color in panel (b). The entanglement of the shortest trefoil-knotted component (U1851–C1892) is shown in panel (c).

fall within, or close to, the range of nucleotides where the model fitting was marked as deviating appreciably from the target electron density map. It is therefore plausible that the unknotted structure obtained by eliminating the essential crossings could provide a better fit to the target em map. This could, in turn, imply that none of the thousands of available RNA structures are knotted.

Further elements in favour of this conclusion arise when comparing the knotted RNAs with other related 23S and 26S units available in the PDB. In particular, besides 2GYA:0 and 1C2W:B there exist 36 other PDB entries of the *Escherichia coli* 23S unit. Strikingly, these alternative structures are all unknotted. They include the 2I2T:B and 2I2V:B chains solved by X-ray at a 3.2Å resolution and the 2GYC:0 cryo-em structure which was solved with same technique used for the knotted 2GYA:0 counterpart, of which it shares the sequence and length. In particular we note that, by applying the ARTS structural alignment[54] algorithm to 2GYA:0 and 2GYC:0 it is found that the two strands 1558-1561 and 1478-1480 which form the essential clasp shown in Fig. 3c for the knotted 2GYA:0 chain, are not interlocked in the unknotted 2GYC:0 structure. It would therefore be interesting to ascertain if the cryo-em data of 2GYA:0 could be better fitted by removing the clasp.

For the 26S ribosomal unit, instead, there exist only two structures in the PDB, including the previously-discussed knotted one for *Thermomyces lanuginosus*. The second structure is for *Tetrahymena thermophila* and is unknotted. This structure was solved by X-ray at a resolution of 3.5Å and its asymmetric unit is split over PDB entries 4A1D:1, 4A18:1, 4A19:1. The two 26S structures, despite differing by knotted state, have very similar sequences. Their mutual sequence identity from a BLASTn alignment[55] is, in fact, 82%. The extensive sequence alignment includes a region encompassing one of the two essential crossings for the knotted 26S structure of *Thermomyces lanuginosus*. The two involved RNA segments, which are interlocked in the *Thermomyces lanuginosus* 26S unit , are unlocked in the *Tetrahymena thermophila* one. Again, towards clarifying the genuine character of the entanglement of the 26S unit knot it could be verified whether removing the interlocking of the two segments improves the cryo-em data fitting.

Regardless of the fact that the pool of knotted RNA entries consists of only three or zero entries, the outcome of the present survey is that the incidence of knots in RNA molecules is utterly negligible both in absolute terms and also by comparison with proteins and viral dsDNA.

Therefore, within the realm of the various "strands of life", RNA seems to be the only instance where physical knots are most rare, and possibly absent altogether.

The striking observation that RNA structures are virtually free of physical knots pose the question of understanding what plausible mechanisms may have ruled out the occurrence of any major type of entanglement in RNA. *A priori* it is possible to envisage several possible selection processes that involve either the kinetics or the thermodynamics of RNA folding.

On the one hand, it is known that the fold organization of naturally-occurring RNA sequences is much simpler than for random sequences with the same overall nucleotide composition. This point is well-illustrated by considering the above-mentioned genus as an indicator of the complexity and entanglement of RNA secondary structures. In fact, one observes that the minimum energy structures of random sequences of $L = 3,000$ nucleotides typically have a genus of the order of $0.13L = 390$ [56] while naturally-occurring ones of the same length have a genus of only 5 to 8. This provides a strong evidence that naturally-occurring RNA sequences have arguably evolved to minimize their geometrical complexity and hence the entanglement of their native folds.

On the other hand, this sequence-encoded simplicity of RNA structures may be further aided by the kinetics of the folding process. In fact, it may be envisaged that the folding of long RNA molecules may occur, at least in part, co-transcriptionally. This mechanism ought to favor the formation of local helices in newly transcribed regions. In this case, it would be very difficult to develop knots in the resulting highly-branched structure of long and helically-folded RNA.

Further clues regarding the relative weight of these two, possibly concurrent mechanisms as well as the functional implications of RNA knots could be provided in the future by the investigation of the newly-discovered eukaryotic circRNAs, where non-trivial structural entanglement is expected to arise from their circularization and could possibly be co-opted to hinder their *in vivo* degradation[42–46].

Finally, we note that the structural properties of the three knotted RNAs suggest how to generalize the strategy previously followed by Seeman and coworkers[57] to design novel RNA sequences capable of self-tying into a fold with 3_1 and 4_1 knots topology. In fact, a possible scheme would be to promote first the formation of a helix and then the threading of its apical loop, as sketched in Fig. 5. As a matter of fact, by increasing the length of the stem one could generate molecular knots of far greater

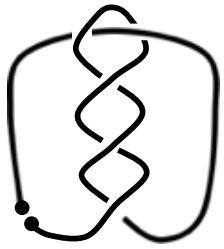

FIG. 5: Design of RNA twist knots. Twist knots (such as the 5_2 knot shown here) can be formed by RNA sequences designed to fold into a helix with an unpaired loop large enough to be threaded by one of the two termini. The knot could be stabilised by base pairing at the clasp (helix apex) or by annealing of the two complementary termini.

complexity than the simplest prime knots achieved so far. This is because by modulating the number of turns in the helix it would be possible to span across the various members of the twist knots, family. The helix length modulation, could be achieved either by increasing the length of the involved sequence, or even by varying the concentration and type of counterions in solution that could affect both the geometry of the helix[57] and the electrostatic persistence length controlling the knot size[58].

III. METHODS

A. RNA structures database

The processed database of RNA chains was obtained by selecting all protein data bank (PDB) entries that contained RNA molecules either alone or complexed/hybridized with other types of biomolecules such as proteins and DNA. Applying such selection criterion to the structures available as of June 2014 returned 2,863 PDB entries, each comprising one or more RNA chains. Of these chains we retained only those that contained RNA nucleotides. Following the criteria adopted by the Jena Library of Biological Macromolecules http://jenalib.fli-leibniz.de/IMAGE.html, this automatic filtering was performed by checking for the presence of at least one nucleotide O2′ atom or of uracil-related residue identifier. Nucleotide entries corresponding to alternate locations in the PDB file are neglected. The resulting structural dataset consisted of 6,394 RNA chains.

B. Detecting and locating knots in RNA chains.

To detect a physical knot in an RNA chain we first bridge the two termini of its backbone (phosphate trace) with a minimally-invasive closing arc [48] so as to obtain a ring. The knotted state of the ring is then established by computing the Alexander determinants and the Dowker code after a topology-preserving simplification of the ring geometry [4, 18, 59]. Applying the topological-profiling scheme to the 6,394 RNA chains returned only nine putatively knotted structures which were further screened for structural integrity. Specifically, to rule out significant structural gaps, we disregarded those chains where consecutive phosphates are farther apart than 15Å. Only the three structures listed in Table 1 were found to have a knotted and gapless backbone. The portions of these chains that accommodate the physical knots (or its separable prime components) were located by using the so-called bottom-up knot search scheme which identifyies the shortest stretch of the phosphate trace that, after closure, has the same desired topology. chain [60].

IV. ACKNOWLEDGMENTS

We thank Giovanni Bussi and Stefano Gustincich for extensive discussions. This work was partially supported by the Italian Ministry of Education grant PRIN No. 2010HXAW77.

[1] P. Virnau, A. Mallam, and S. Jackson, J Phys: Condens Matter **23**, 033101 (2011).
[2] A. Eriksson, T. Jones, and A. Liljas, Proteins **4**, 274 (1988).
[3] M. Mansfield, Nat Struct Biol **1**, 213 (1994).
[4] Taylor, WR, Nature **406**, 916 (2000).
[5] N. King, E. Yeates, and T. Yeates, J Mol Biol **373**, 153 (2007).
[6] R. Potestio, C. Micheletti, and H. Orland, PLoS Comput Biol **6**, e1000864 (2010).
[7] D. Bölinger, J. Sulkowska, H. Hsu, L. Mirny, M. Kardar, J. Onuchic, and P. Virnau, PLoS Comput Biol **6**, e1000731 (2010).
[8] P. Virnau, L. Mirny, and M. Kardar, PLoS Comput Biol **2**, e122 (2006).
[9] J. Sulkowska, E. Rawdon, K. Millett, J. Onuchic, and A. Stasiak, Proc Natl Acad Sci USA **109**, E1715 (2012).
[10] A. Mallam and S. Jackson, Nat Chem Biol **8**, 147 (2012).
[11] S. Wallin, K. Zeldovich, and E. Shakhnovich, J Mol Biol **368**, 884 (2007).
[12] J. I. Sulkowska, P. Sulkowski, and J. Onuchic, Proc Natl Acad Sci USA **106**, 3119 (2009), ISSN 1091-6490.
[13] S. a Beccara, T. Skrbic, R. Covino, C. Micheletti, and P. Faccioli, PLoS Comput Biol **9**, e1003002 (2013).
[14] R. Lua and A. Grosberg, PLoS Comput Biol **2**, e45 (2006).
[15] D. Sumners and S. Whittington, J Phys A: Math Gen **21**, 1689 (1988).
[16] C. Micheletti, D. Marenduzzo, E. Orlandini, and D. Sumners, Biophys J **95**, 3591 (2008).
[17] D. Meluzzi, D. Smith, and G. Arya, Annu Rev Biophys **39**, 349 (2010).
[18] C. Micheletti, D. Marenduzzo, and E. Orlandini, Phys Rep **504**, 1 (2011).
[19] L. Liu, L. Perkocha, R. Calendar, and J. Wang, Proc Natl Acad Sci USA **78**, 5498 (1981).
[20] J. Menissier, P. Laquel, G. Lebeurier, and L. Hirth, Nucleic Acids Res **12**, 8769 (1984).
[21] J. Arsuaga, M. Vázquez, S. Trigueros, D. Sumners, and J. Roca, Proc Natl Acad Sci USA **99**, 5373 (2002).
[22] Arsuaga, J and Vázquez, M and McGuirk, P and Trigueros, S and Sumners, DW and Roca J, Proc Natl Acad Sci USA **102**, 9165 (2005).
[23] S. Trigueros and J. Roca, BMC Biotechnol **7**, 94 (2007).
[24] V. Rybenkov, N. Cozzarelli, and A. Vologodskii, Proc Natl Acad Sci USA **90**, 5307 (1993).
[25] D. Marenduzzo, E. Orlandini, A. Stasiak, D. Sumners, L. Tubiana, and C. Micheletti, Proc Natl Acad Sci USA

106, 22269 (2009).
[26] A. Vologodskii, W. Zhang, V. Rybenkov, A. Podtelezhnikov, D. Subramanian, J. Griffith, and N. Cozzarelli, Proc Natl Acad Sci USA **98**, 3045 (2001).
[27] Z. Liu, L. Zechiedrich, and H. S. Chan, J Mol Biol **400**, 963 (2010).
[28] A. Rosa, M. Di Ventra, and C. Micheletti, Phys Rev Lett **109**, 118301 (2012).
[29] D. Marenduzzo, C. Micheletti, E. Orlandini, and D. Sumners, Proc Natl Acad Sci USA **110**, 20081 (2013).
[30] N. King, A. Jacobitz, M. Sawaya, L. Goldschmidt, and T. Yeates, Proc Natl Acad Sci USA **107**, 20732 (2010).
[31] W. Shih and C. Lin, Curr Opin Struct Biol **20**, 276 (2010).
[32] J. Tang, N. Du, and P. Doyle, Proc Natl Acad Sci USA **108**, 16153 (2011).
[33] D. Marenduzzo, C. Micheletti, and E. Orlandini, Physics World **Apr.**, 30 (2013).
[34] K. Rietveld, R. Van Poelgeest, C. Pleij, J. Van Boom, and L. Bosch, Nucleic Acids Res **10**, 1929 (1982).
[35] K. Rietveld, C. Pleij, and L. Bosch, EMBO J **2**, 1079 (1983).
[36] D. Giedroc, C. Theimer, and P. Nixon, J Mol Biol **298**, 167 (2000).
[37] S. Cho, D. Pincus, and D. Thirumalai, Proc Natl Acad Sci USA **106**, 17349 (2009).
[38] G. Chen, K. Chang, M. Chou, C. Bustamante, and I. Tinoco, Proc Natl Acad Sci USA **106**, 12706 (2009).
[39] T. Hansen, S. Reihani, L. Oddershede, and M. Sorensen, Proc Natl Acad Sci USA **104**, 5830 (2009).
[40] D. Ritchie, D. Foster, and M. Woodside, Proc Natl Acad Sci USA **109**, 16167 (2012).
[41] H. Wang, R. Di Gate, and N. Seeman, Proc Natl Acad Sci USA **93**, 9477 (1996).
[42] J. Salzman, C. Gawad, P. Wang, N. Lacayo, and P. Brown, PloS one **7**, e30733 (2012).
[43] S. Memczak, M. Jens, A. Elefsinioti, F. Torti, J. Krueger, A. Rybak, L. Maier, S. Mackowiak, L. Gregersen, M. Munschauer, et al., Nature **495**, 333 (2013).
[44] W. Jeck, J. Sorrentino, K. Wang, M. Slevin, C. Burd, J. Liu, W. Marzluff, and N. Sharpless, RNA **19**, 141 (2013).
[45] J. Salzman, R. Chen, M. Olsen, P. Wang, and P. Brown, PLoS Genet **9**, e1003777 (2013).
[46] M. Frank-Kamenetskii, Artificial DNA: PNA & XNA **4**, 35 (2013).
[47] H. Berman, T. Bhat, P. Bourne, Z. Feng, G. Gilliland, H. Weissig, and J. Westbrook, Nature Struct Biol **7 Suppl**, 957 (2000).
[48] L. Tubiana, E. Orlandini, and C. Micheletti, Progr Theor Exp Phys **191**, 192 (2011).
[49] H. Orland and A. Zee, Nucl Phys B **620**, 456 (2002).
[50] M. Bon, G. Vernizzi, H. Orland, and A. Zee, J Mol Biol **379**, 900 (2008).
[51] M. Bon and H. Orland, Nucleic Acids Res **39**, e93 (2011).
[52] M. Bon, C. Micheletti, and H. Orland, Nucleic Acids Res **41**, 1895 (2013).
[53] M. Antczak, T. Zok, M. Popenda, P. Lukasiak, R. Adamiak, J. Blazewicz, and M. Szachniuk, Nucleic Acids Res **42**, W368 (2014).
[54] O. Dror, R. Nussinov, and H. Wolfson, Nucleic Acids Res **34**, W412 (2006).
[55] S. Altschul, T. Madden, A. Schäffer, J. Zhang, Z. Zhang, W. Miller, and D. Lipman, Nucleic Acids Res **25**, 3389 (1997).
[56] G. Vernizzi, P. Ribeca, H. Orland, and A. Zee, Phys Rev E **73**, 031902 (2006), ISSN 1539-3755.
[57] N. Seeman, Acc Chem Res **30**, 357 (1997).
[58] P. Dommersnes, Y. Kantor, and M. Kardar, Phys Rev E **66**, 031802 (2002).
[59] K. Koniaris and M. Muthukumar, Phys Rev Lett **66**, 2211 (1991).
[60] L. Tubiana, E. Orlandini, and C. Micheletti, Phys Rev Lett **107**, 188302 (2011).